Catalysis Today 175 (2011) 141–146

Contents lists available at ScienceDirect

Catalysis Today

journal homepage: www.elsevier.com/locate/cattod

Efficient simulation of an ammonia oxidation reactor using a solution mapping approach

A. Scheuer[a,b], O. Hirsch[b,c], R. Hayes[c], H. Vogel[a], M. Votsmeier[b,*]

[a] Ernst-Berl Institut, TU-Darmstadt, Petersenstr. 20, 64287 Darmstadt, Germany
[b] Umicore AG & Co. KG, Rodenbacher Chaussee 4, 63457 Hanau, Germany
[c] Department of Chemical and Materials Engineering, University of Alberta, Edmonton, AB, Canada T6G 2G6

ARTICLE INFO

Article history:
Received 4 November 2010
Received in revised form 2 March 2011
Accepted 14 March 2011
Available online 13 April 2011

Keywords:
Catalysis
Spline
Mapping
Diffusion
Ammonia oxidation
Mechanistic kinetics

ABSTRACT

A highly efficient single channel monolith reactor model for the oxidation of ammonia is implemented. A mechanistic model for ammonia oxidation on platinum is used, and all internal and external mass transfer effects are included. The model efficiency is derived from the use of pre-computed solutions of the mass balance equations. Spline interpolation functions are constructed from pre-computed solutions of the mass balances of one volume element of the reactor model. It is shown that these spline functions reproduce the exact outlet concentrations of the volume element with a relative error of less than 3%. This solution mapping approach allows computation of concentration profiles in the reactor by simple successive calls of the interpolation function without any numerical solution. Outlet concentrations of the complete reactor computed in this way show a relative error of less than 2%. Application of the solution mapping approach speeds up the solution of the concentration profiles by a factor of more than 3200, compared to the numerical solution of the mass balances. In this way one steady state concentration profile in an ammonia oxidation catalyst can be computed in less than 0.003 s, despite the fact that the model uses mechanistic surface kinetics and includes the radial diffusion in the washcoat.

1. Introduction

The control of emissions of nitric oxides (NO_X) is a significant problem in most combustion processes, and is difficult in a system containing significant amounts of oxygen. Although there are several possible solutions, the selective catalytic reduction (SCR) using ammonia (NH_3-SCR) is one proven technique. In this system, ammonia is added to the exhaust in the form of an aqueous urea solution. One drawback of this method is that ammonia may pass through the system without reacting, which is called ammonia slip. Ammonia has a strong odour, and therefore a suitable means must be found to eliminate this slippage. To achieve this goal, recent SCR systems use an ammonia oxidation catalyst (also known as an ammonia slip catalyst) downstream of the SCR catalyst, whose purpose is the destruction of excess ammonia. Not only does this catalyst reduce or eliminate ammonia slip, but it can also lead to a better performance of an SCR catalyst by allowing a more aggressive dosing strategy.

First generation ammonia slip catalysts consisted of platinum supported on an alumina formulation. Kraehnert et al. [1] developed a surface kinetic model for conditions used in the Ostwald process using platinum foil. This model was subsequently reparameterized for an automotive Pt/Al_2O_3 catalyst by Scheuer et al. [2]. In [3] this mechanism was implemented in a 2D model of a monolith channel. Owing to the high space velocities under typical operating conditions of ammonia slip reactors, mass transfer to and within the washcoat plays a significant role in these catalysts. Realistic reactor models must therefore include the diffusion effects in the washcoat, which adds considerably to the computational cost.

The washcoat distribution in a real channel is non-uniform which can cause variations in both the external and the internal mass transfer [4,5]. Typically, a reactor model for a single channel is, at a minimum, reduced to a two dimensional one by treating the system as axi-symmetric. Because such models can still be expensive, further approximations are often made. The most common approach to implement radial diffusion effects in a reactor model is to solve for the axial concentration profiles in 1D and to couple this solution with a second 1D solution that at each position solves the radial reaction diffusion equation. Such so-called 1D + 1D models have also been used in combination with mechanistic surface kinetics [6,7]. However, these simulators still require long computation times, and the application of these programs seems to be limited to a few published demonstration studies.

One method that can be used to reduce the execution time for models using mechanistic kinetic models is to pre-compute the rate

* Corresponding author at:Umicore AG & Co. KG, Rodenbacher Chaussee 4 63457 Hanau-Wolfgang Germany, Tel.: +496181594252.
E-mail address: martin.votsmeier@eu.umicore.com (M. Votsmeier).

0920-5861/$ – see front matter © 2011 Published by Elsevier B.V.
doi:10.1016/j.cattod.2011.03.036

Table 1
Network of ammonia oxidation reaction according to Scheuer et al. [2]. The mechanism assumes two different types of active sites, denoted as a and b.

No.	Reaction	Equation
R1	NH_3 adsorption	$NH_3 + b \rightarrow NH_3\text{-}b$
R2	NH_3 desorption	$NH_3\text{-}b \rightarrow NH_3 + b$
R3	O_2 adsorption	$O_2 + 2a \rightarrow 2O\text{-}a$
R4	O_2 desorption	$2O\text{-}a \rightarrow O_2 + 2a$
R5	NH_3 activation	$NH_3\text{-}b + 1.5O\text{-}a \rightarrow N\text{-}a + 1.5H_2O + 0.5a + b$
R6	NO desorption	$NO\text{-}a \rightarrow NO + a$
R7	NO adsorption	$NO + a \rightarrow NO\text{-}a$
R8	N_2 formation	$2N\text{-}a \rightarrow N_2 + 2a$
R9	NO formation	$N\text{-}a + O\text{-}a \rightarrow NO\text{-}a + a$
R10	N_2O formation	$NO\text{-}a + N\text{-}a \rightarrow N_2O + 2a$

data over the expected range of temperature and concentration. We have previously shown that mechanistic surface kinetics can be efficiently implemented in reactor models by a spline interpolation of such pre-computed rate data [3,8]. This rate mapping approach involves a pre-processing step where the surface rate equations are solved for a large number of catalyst operating conditions. From these data a spline interpolation function is built. During the execution of the simulation the source terms for the gas species can be efficiently computed by a simple call to the interpolation function.

The basic implementation of pre-computed rate data still requires that a numerical solver is used for the computation of concentration profiles in the monolith. The approach of the current paper is to build an interpolation function that maps the solution for an individual reactor volume element. We build an interpolation function that represents the solution of one volume element of the 1D + 1D model. In this way not only the surface kinetics, but also the diffusion limitations in the washcoat and gas-wall mass transfer are included in the mapping. This allows the computation of concentration profiles in a reactor by simple successive calls of the interpolation function without any numerical solution procedure. It is shown that this solution mapping approach allows the implementation of ammonia oxidation kinetics in a 1D + 1D type model with a speedup by a factor of 3200, compared to the numerical solution of the 1D + 1D model. In this way one steady state concentration profile in an ammonia oxidation catalyst can be computed in less than 0.003 s, despite the fact that the model uses mechanistic surface kinetics and includes the radial diffusion in the washcoat.

2. Methodology

2.1. Numerical model

The reactor model used in this work is isothermal and describes one representative channel of the monolith. The channel is discretized in the axial direction and concentration profiles along the channel are computed by successive solution of the mass balance for each of the volume elements. The same subroutines as used for the numerical computation of the concentration profiles are also applied for the construction of the look-up tables. Section 2.1.2 discusses the mass balance equations for a 1D model that ignores diffusion effects in the washcoat. Section 2.1.3 presents the mass balance equations for a 1D + 1D model that takes into account the radial concentration gradients in the washcoat.

2.1.1. Rate equations

The kinetics of the ammonia oxidation is represented by the surface kinetic model of Scheuer et al. [2] developed on a Pt/Al_2O_3 catalyst shown in Table 1. The parameters are valid for a gas composition of 0–600 ppm NH_3, 0–300 ppm NO, 6% O_2, 5% H_2O and 300 000 h^{-1} GHSV.

The individual reaction rate r of reaction k is computed by:

$$r_k = \Gamma k_{0k} \exp\left(-\frac{E_{ak}}{RT}\right) \prod_i \theta_i^{|\nu_{ik}|} \prod_i c_i^{|\nu_{ik}|} \quad (1)$$

where c_i is the concentration of gas phase species i, θ_i is the surface coverage of the surface species i and ν_{ik} is the stoichiometric coefficient of species i in reaction k. The pre-exponential factors k_{0k} and the activation energy E_{ak} of reaction k are taken from Scheuer et al. [2]. With the individual reaction rate terms known, the overall source term $\dot{s}$ for species i is calculated by:

$$\dot{s}_i = \sum_k \nu_{ik} r_k \quad (2)$$

2.1.2. Mass balances for the 1D model (without washcoat diffusion)

This 1D model solves the mass balances for the open channel and assumes that all of the reaction occurs at the surface of the washcoat. Assuming plug flow and uniform velocity, the transient mass balance for the open channel is:

$$\frac{dc_{i\,gas}}{dt} = -v\frac{dc_{i\,gas}}{dz} - \frac{4\beta_i}{d}(c_{i\,gas} - c_{i\,wc}) \quad (3)$$

where v is the average gas velocity, $c_{i\,gas}$ is the concentration of the gas phase species i and $c_{i\,wc}$ is the concentration at the washcoat surface. The spatial derivative can be discretized using an upwind formulation, and the result expressed in terms of the residence time τ of the fluid in the volume element, giving:

$$\frac{dc_{i\,gas}}{dt} = \frac{c_{i\,gas\,in} - c_{i\,gas}}{\tau} - \frac{4\beta_i}{d}(c_{i\,gas} - c_{i\,wc}) \quad (4)$$

where $c_{i\,gas\,in}$ is the concentration of the entering gas from the upstream direction and d the diameter of the monolith channel. β_i is the mass transfer coefficient of species i, computed from the Sherwood Number:

$$\mathrm{Sh} = \frac{\beta_i d}{D_i} \quad (5)$$

where D_i is the diffusion coefficient of species i in nitrogen. A position independent Sherwood number of Sh = 3.66 was used in this work. In reality the mass transfer coefficient is higher at the inlet of the channel due to the developing velocity and concentration boundary layers. We tested a correlation from [9] that takes into account the effect of developing concentration profiles by a position dependent mass transfer coefficient. Our calculations show that for the conditions treated in this study the application of a position independent mass transfer coefficient leads to negligible errors in the output concentrations.

The mass balances for the gas species in the washcoat are

$$\frac{dc_{i\,wc}}{dt} = \frac{4\beta_i}{d}(c_{i\,gas} - c_{i\,wc}) + \dot{s}_i \quad (6)$$

The balances for the surface species are

$$\frac{d\theta_i}{dt} = \frac{\dot{s}_i}{\Gamma} \quad (7)$$

where Γ is the concentration of active sites.

Steady state was assumed for the gas phase concentrations in the open channel state ($dc_{i\,gas}/dt = 0$) and in the washcoat ($dc_{i\,wc}/dt = 0$). The resulting system of equations is numerically integrated using the solver package DASSL [10] until a steady state for the surface species is obtained.

2.1.3. Mass balances for the 1D + 1D model (including washcoat diffusion)

The 1D + 1D model discretizes the washcoat in radial volume elements and solves the mass balances for the open channel and

Table 2
Input variables for the spline map and parameter range.

	Lower boundary	Upper boundary
T [K]	300	800
x_{NH_3} [mol mol^{-1}]	1×10^{-8}	1×10^{-3}
x_{NO} [mol mol^{-1}]	1×10^{-8}	1×10^{-3}
x_{O_2} [mol mol^{-1}]	0.02	0.2
τ [ms]	4.8×10^{-2}	0.8

each of the washcoat volume elements. The mass balance for the open channel is the same as for the 1D model (Eq. (4)). The mass balances for the gas species of the radial washcoat elements are

$$\frac{dc_{i\,wc\,n}}{dt} = \frac{J_{i\,n} - J_{i(n+1)}}{d_n} + \dot{s}_{i\,n} \tag{8}$$

and for the surface species

$$\frac{d\theta_{i\,n}}{dt} = \frac{\dot{s}_{i\,n}}{\Gamma} \tag{9}$$

where $c_{i\,wc\,n}$ is the concentration of gas species i in the radial washcoat element n and d_n is the diameter of the washcoat element n. J_{in} ($n \geq 1$) is the flux of gas species i from the $(n-1)$th to the nth cell. The fluxes between two cells are calculated according to Fick's law:

$$J_{i\,n} = (c_{i\,wc\,(n-1)} - c_{i\,wc\,n}) \frac{D_{eff}}{d_{wc\,(n-1)}} \quad \text{for} \quad n \geq 2 \tag{10}$$

where D_{eff} is the effective diffusion coefficient estimated as 1×10^{-6} m^2 s^{-1} at 300 K [11] and $d_{wc\,(n-1)}$ is the thickness of the $(n-1)$th volume element.

$J_{i\,1}$ is the flux from the open channel (formally: $n = 0$) to the first washcoat element. It is computed based on a mass transfer coefficient:

$$J_{i\,1} = \frac{4\beta_i}{d}(c_{i\,gas} - c_{i\,wc\,1}) \tag{11}$$

The resulting system of differential algebraic equations is integrated in time by the numerical solver DASSL [10] until steady state is reached.

2.2. The spline mapping

The purpose of the spline mapping is to describe the output concentrations of one volume element as a function of the volume element's inlet concentrations, temperature and residence time. In this way, the spline mapping allows computation of a concentration profile in the monolith reactor by simple successive calls of the interpolation function without application of a numerical solver.

To construct the spline functions, the mass balances for one reactor volume element must be solved for a large number of input conditions. Construction of a tensor product spline requires that the input data be located on a rectangular grid. The number of data points in each direction can be freely chosen (see Section 2.2.4). Table 2 presents the input range for each of the five input parameters of the spline map.

2.2.1. Scaling of the input data for the spline interpolation

The accuracy of a spline interpolation can be improved by an appropriate scaling of the data. Two different types of scaling were used here, first a direct logarithmic scaling of the volume element's outlet concentration, and secondly a mapping of the effective source terms for the volume element.

2.2.1.1. Mapping of the volume elements output concentration. The outlet concentrations of NH_3 and NO are mapped using a logarithmic scaling. According to the reaction mechanism used here, the concentrations of N_2 and N_2O have no influence on the rates of NH_3 consumption or product formation. For this reason, the concentrations of N_2 and N_2O do not need to be considered as input species of the spline map. Rather, for these two species, instead of the outlet concentration, the logarithm of the concentration change in the volume element is mapped in the spline function.

Table 3
Comparison of the interpolation time for various number of parallel calls between commercially available Matlab code and the same code implemented into a Fortran routine.

No. of parallel calls	Matlab	Fortran	Speed-up
1	1.90×10^{-3}	3.38×10^{-5}	56.4
10	2.96×10^{-3}	2.39×10^{-4}	12.4
100	1.12×10^{-2}	2.57×10^{-3}	4.38
1000	1.65×10^{-1}	2.68×10^{-2}	6.17

2.2.1.2. Mapping of the volume elements effective source term. Effective source terms $\dot{s}_{i\,eff}$ are computed based on the solution of the mass balance of the volume element according to

$$\dot{s}_{i\,eff} = \frac{c_{i\ \ gasin} - c_{i\ \ gasout}}{\tau} \tag{12}$$

where $c_{i\,gas\,in}$ and $c_{i\,gas\,out}$ are the inlet and outlet concentration of species i and τ is the residence time in the volume element. The effective source term of NH_3, N_2 and N_2O are mapped as their logarithms. For NO the effective source term assumes positive and negative values so that the logarithmic scaling cannot be applied in this case.

During the interpolation procedure the outlet concentrations of each volume element are computed from the interpolated effective source terms according to Eq. (12).

2.2.2. Construction and evaluation of the spline functions

Multi-dimensional tensor-spline functions were constructed using the toolbox of De Boor [12]. To allow for a fast evaluation, the spline functions are represented in the so-called polynomial form. This means that the coefficients of the polynomials for the individual grid elements are stored during data pre-processing, so that during the interpolation operation only the polynomial needs to be evaluated.

In our earlier work we used a Matlab implementation of De Boors toolbox for the evaluation of the spline functions [3,8]. In this the work the spline evaluation has been implemented in Fortran. Due to the computational overhead associated with the Matlab language, the Fortran implementation is faster by a factor of 5–50 (see Table 3). The advantage of the Fortran implementation is largest if the interpolation routine is called for an individual data point. Simultaneous computation of several data points reduces the overhead of the Matlab implementation but the Fortran code remains faster by factor 5 even for large input arrays.

2.2.3. Error estimation

A validation test set consisting of 10 000 data points, randomly sampled from the input space of the mapping, was calculated to determine the quality of the spline representation. Therewith we test the accuracy and validity of the method for large number of different gas compositions.

Two different error criteria are used and combined for measuring the performance of the spline approximation.

The first criterion e_1 is the relative error calculated as:

$$e_1 = \frac{|x - x_{spline}|}{x} \tag{13}$$

with x as the mole fraction calculated by the numerical solver and x_{spline} as the mole fraction calculated by the spline representation.

If the output concentration becomes small, very small absolute errors can lead to a large relative error in the output concentration. For this reason a second error criterion in form of a scaled absolute error is used:

$$e_2 = \frac{|x - x_{spline}|}{x_{threshold}} \tag{14}$$

The threshold mole fraction $x_{threshold}$ is chosen as 1 ppm. This means that for output concentrations below 1 ppm the scaled absolute error e_2 is larger than the relative error. A combined error criterion uses the lower error of Eq. (13) and (14) and is calculated by:

$$e_{total} = \sqrt{\frac{1}{N}\sum_{N} \min(e_1, e_2)^2} = \sqrt{\frac{1}{N}\sum_{N} \left(\frac{|x - x_{spline}|}{\max(x, x_{threshold})}\right)^2} \tag{15}$$

2.2.4. Optimization of the lookup table

The number of grid points needed in every single input dimension was adapted following the procedure reported in [8].

The starting point was a grid with two points in every dimension. An error between the spline-interpolated and the correct values of the numerical solver was calculated according to Eq. (15).

Each iteration of the optimization increases the number of steps in each dimension separately. The direction of the best average error is used for the next step.

The new grid points were chosen such that every new point is in between two existing points. The next number of grid points in one certain dimension has always $n_{next} = 2n - 1$ points, with n as number of the current points. Starting with two input points per dimension, the next steps would be three, five and nine. This method was used with one certain space velocity. In a last step the space velocity was varied and added to this lookup table.

3. Results and discussion

3.1. Mapping the outlet mole fractions vs. effective source terms

The straightforward representation of the conversion efficiency for an individual reactor volume element is a direct mapping of the outlet concentrations. An alternative procedure is to compute effective reaction source terms in the volume element and to interpolate these effective rates by the spline mapping (see Section 2.2). The purpose of this section is to compare both mapping strategies systematically. To this end, maps with identical input dimensions were constructed using both strategies. These maps have a reduced input dimension and only use temperature (25 grid points) and the mole fractions of NH_3 and NO (20 grid points) as input parameters. The residence time τ for the full monolith and the oxygen concentration were kept at fixed values of 12 ms and 6%, respectively. Furthermore, for the comparison presented in this section the simplified 1D reactor model (Section 2.1.2) that does not take into account concentration gradients in the washcoat was used.

Table 4 compares the interpolation accuracy of the outlet concentrations for a single volume element and a full monolith computed by both mapping strategies. Obviously, both strategies show a similar performance if one compares the error in the output of an individual volume element. For the remaining part of this paper we use a mapping of the effective source terms, because it has been found that this approach yields slightly smaller interpolation errors, if one compares the errors at the outlet of a complete reactor.

3.2. Optimizing the size of the spline map

In a next step the more complex numerical model including washcoat diffusion was used as basis for the creation of the spline map. To find a suitably sized and sufficiently accurate spline function, the number of grid points in each input dimension was optimized as described in Section 2.2.4. This optimization is done for a fixed residence time so that the optimized spline function is 4-dimensional, with the input dimensions temperature and the input mole fractions of NH_3, NO and O_2.

Table 4
Comparison of the relative error according to Section 2.2.3 for different orders of spline functions and for the methods of mapping either the mole fraction or the source term. The errors are shown for the solution of a single monolith channel, with a residence time of 12/25 ms, and for the solution of a full monolith consisting of 25 channels.

	Mole fraction mapped			Rates mapped		
	Linear (%)	Quadratic (%)	Cubic (%)	Linear (%)	Quadratic (%)	Cubic (%)
Single volume element						
NH_3	0.45	0.44	0.44	0.46	0.44	0.44
N_2	4.14	3.52	3.52	4.14	3.52	3.51
N_2O	3.44	2.80	2.80	3.44	2.80	2.80
NO	1.98	1.83	1.83	1.52	1.83	1.83
Full monolith consisting of 25 elements						
NH_3	1.40	0.72	0.69	1.74	0.64	0.63
N_2	1.86	0.54	0.52	1.54	0.51	0.50
N_2O	1.10	0.28	0.27	0.99	0.27	0.26
NO	2.33	0.46	0.44	1.59	0.46	0.44

Fig. 1 shows the evolution of the number of grid elements in the different input directions during the adaptive spline construction. The final spline map uses 17 grid elements for temperature, 9 grid elements for NH_3 and NO and only 3 grid elements for the oxygen input mole fraction.

Fig. 2 shows the average error of the output concentrations during the optimization procedure. While the difference between cubic and quadratic spline order is not significant, the error of both is significantly smaller than for the linear spline. As the storage space strongly increases with the order of the polynomial, a quadratic order of the spline is used in the work presented in the remaining part of this paper.

In a final step the residence time in the volume element was added as the fifth input dimension of the interpolation function. Preliminary tests had shown that the influence of the residence time can well be captured by a linear spline. For this reason a polynomial order of one was chosen for this input dimension. The number of input points in this dimension was successively increased. The final spline function uses 11 data points for the space velocity. The relative interpolation error for the final 5-dimensional

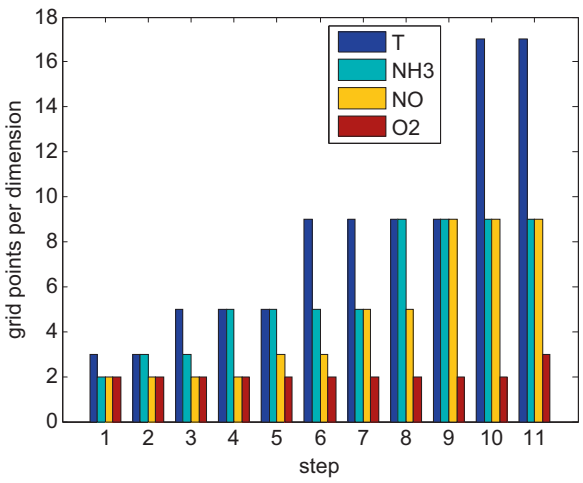

Fig. 1. Number of grid points in each dimension against the step number of the optimization routine.

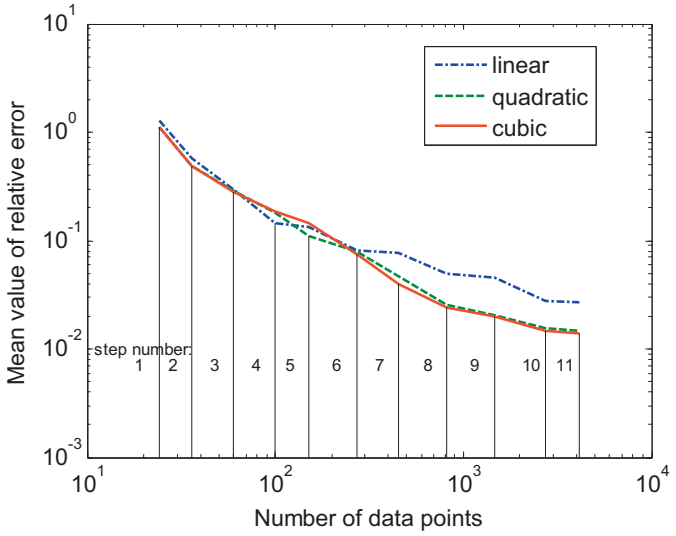

Fig. 2. The average error of the output mole fractions according to Eq. (15) is plotted against the total number of grid points used for the map. The logarithm of the source term is the mapped value.

spline representation of the outlet concentrations for one reactor volume element is reported in Table 5.

3.3. Validation of the solution mapping approach in reactor simulations

To demonstrate the performance of the solution mapping approach in full reactor simulations, concentration profiles were computed by numerical solution of the 1D + 1D model and by successive calls of the spline interpolation function. All of these simulations use a discretization with 25 axial volume elements. Fig. 3 shows the outlet concentrations of NH_3, N_2, N_2O and NO as a function of inlet temperature. Obviously, the results of the full numerical solution of the 1D + 1D model are perfectly reproduced by the spline mapping approach.

To provide a more statistically valid measure of the accuracy of the rate mapping approach for full monolith simulations, calculations were performed for a test set of 10 000 input conditions samples taken randomly from the input range of Table 2. Table 5 presents the average error for the different output species. The average error for the concentrations at the outlet of the full monolith is below 2% for all species.

Table 6 compares the runtime performance (Intel Xeon X5355 at 2.66 GHz) of the solution mapping approach and the numerical solution of the 1D + 1D model. Application of the solution mapping leads to a speed up of 3200 compared to the conventional numerical solution.

Table 5
Relative error of the solution mapping approach for the solution of a full monolith channel (25 cells) and the errors of the first cell. A test set of 10 000 data points has been sampled randomly from the input space of Table 2 Relative errors have been computed according to Eq. (15).

	Full monolith		First cell	
	Rate mapped	Mole fraction mapped	Rate mapped	Mole fraction mapped
NH_3	0.59	0.86	0.18	0.18
N_2	1.35	1.90	2.79	3.00
N_2O	0.94	1.54	2.23	2.54
NO	1.36	1.20	1.57	1.71

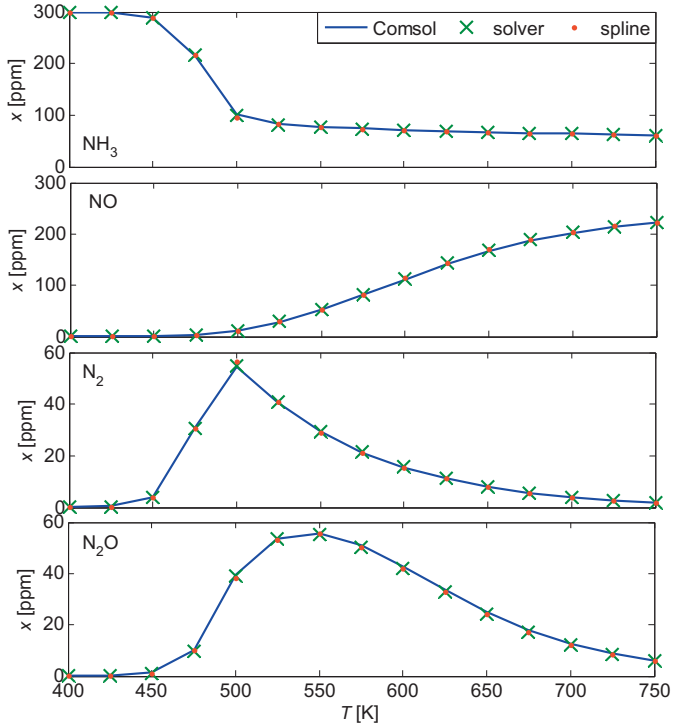

Fig. 3. Mole fractions at reactor outlet are plotted against temperature. Data from the calculations published in [3] are compared to spline data and numerical data from the current work. Reaction conditions are 300 ppm NH_3, 6% O_2 and a SV of 300 000 h^{-1}.

Table 6
Calculation times for the results of Table 5. The reported computation times are for the computation of one concentration profile with the 1D + 1D model (axial discretization: 25 volume elements).

Numerical solver	Spline interpolation	Speed up
9.861 s	0.003 s	3287

3.4. Comparison with full 2D solution of the concentration profile

Finally, the results of the 1D + 1D model of this work are compared to a numerical solution of the full 2D concentration profiles in an axi-symmetric monolith channel. Such results have been presented in [3] using the software package Comsol. The results of the full 2D solution are included in Fig. 3. The results of the numerical solver agree extremely well with the Comsol calculations. This shows that the approximations applied in the 1D + 1D model (representation of gas phase diffusion by a position independent mass transfer coefficient, neglect of axial diffusion) have little effect on the model's accuracy.

4. Conclusion

In previous work we have shown that complex mechanistic kinetics can be efficiently implemented in reactor simulations by a spline mapping of pre-computed source terms for the gas species. This so-called rate mapping still requires a numerical solver for the computation of the concentration profiles. In this work we show that the computational efficiency can be further enhanced if the complete solution of the mass balances (including diffusion in washcoat) for an individual reactor volume element is mapped by a spline function.

The approach is demonstrated using a 1D + 1D model of an ammonia slip catalyst with mechanistic kinetics. The spline interpolation reproduces the numerical solution for the output con-

centrations of an individual volume element with an accuracy of better than 3%. The outlet concentrations of an entire reactor with 25 axial volume elements are reproduced with an accuracy of better than 2%. Application of the solution mapping approach speeds up the calculation of concentration profiles in a reactor by a factor of more than 3200, compared to a numerical solution of the mass balances. This means that now a model for one monolith channel that uses mechanistic surface kinetics and includes radial diffusion in the washcoat can be solved in less than 0.003 s.

Such ultra-fast simulators will enable new applications of simulation in areas that require repetitive solution of the catalyst model such as model predictive control, model based system optimization or implementation of catalyst models in 3D CFD simulations.

Acknowledgements

This project was completed under the auspices of the AUTO21 NCE program, project D305-DCC, and the authors are grateful for this support. The assistance of Teng-Wang Nien of the Department of Chemical and Materials Engineering, University of Alberta is also acknowledged.

References

[1] R. Kraehnert, M. Baerns, Chem. Eng. J. 137 (2008) 361–375.
[2] A. Scheuer, M. Votsmeier, A. Schuler, J. Gieshoff, A. Drochner, H. Vogel, Top. Catal. 52 (2009) 1847–1851.
[3] M. Votsmeier, A. Scheuer, A. Drochner, H. Vogel, J. Gieshoff, Catal. Today 151 (2010) 271–277.
[4] R.E. Hayes, B. Liu, R. Moxom, M. Votsmeier, Chem. Eng. Sci. 59 (2004) 3169–3181.
[5] R.E. Hayes, B. Liu, M. Votsmeier, Chem. Eng. Sci. 60 (2005) 2037–2050.
[6] P. Koci, M. Kubicek, M. Marek, Ind. Eng. Chem. Res. 43 (2004) 4503–4510.
[7] R. Hayes, L. Mukadi, M. Votsmeier, J. Gieshoff, Top. Catal. 30/31 (2004) 411–415.
[8] M. Votsmeier, Chem. Eng. Sci. 64 (2009) 1384–1389.
[9] E. Tronconi, P. Forzatti, AIChE J. 38 (1992) 201–210.
[10] K.E. Brenan, S.L. Campbell, L.R. Petzold, Numerical Solution of Initial-Value Problems in Differential-Algebraic Equations, Elsevier Science Publishing Co., New York, 1989.
[11] F. Zhang, R.E. Hayes, S.T. Kolaczkowski, Chem. Eng. Res. Des. Trans. IChemE: Part A 82 (2004) 481–489.
[12] C. De Boor, A Practical Guide to Splines, Springer, New York, 1978.